Crestal Bone Changes at Nonsubmerged Implants (Camlog) with Different Machined Collar Lengths: A Histomorphometric Pilot Study in Dogs

Frank Schwarz, DDS, Dr Med Dent, PhD[1]/Monika Herten, Dr Rer Nat[2]/
Katrin Bieling, DDS, Dr Med Dent[2]/Jürgen Becker, DDS, Dr Med Dent, PhD[3]

Purpose: *The aim of the present study was to histomorphometrically investigate crestal bone changes at nonsubmerged implants (Camlog) with different machined collar lengths in a dog model.* ***Materials and Methods:*** *One-stage insertion of sandblasted acid-etched screw-type implants with machined neck sizes of 1.6 mm (CAM) and 0.4 mm (CAM+) was performed in the mandibles of 4 beagle dogs. Both types of implants were inserted so that the implant shoulder (IC) exceeded the alveolar crest for 0.4 mm. Placement was followed by the connection of standard abutments. The animals were sacrificed after 2 and 12 weeks. Dissected blocks were processed for histomorphometric analysis (eg, distance between IC and the coronal extension of bone-implant contact [CBI], the distance between IC and the apical extension of the inflammatory cell infiltrate, and the percentage of bone-implant contact).* ***Results:*** *Histomorphometric analysis revealed significantly increased mean IC-CBI (CAM: 2.4 ± 0.3 mm; CAM+: 1.6 ± 0.1 mm) and BIC (CAM: 77%; CAM+: 80%) values in both groups at 12 weeks. However, mean IC-CBI values were significantly higher in the CAM group (*P < .01*). An inflammatory cell infiltrate was localized to the implant-abutment interface of both CAM and CAM+ implants, and BC was clearly separated from aICT by a subepithelial connective tissue zone.* ***Conclusions:*** *Within the limits of the present study, it was concluded that* (1) *rough-surfaced implant necks reduced crestal bone level changes after 12 weeks of healing, and* (2) *microbial leakage apparently did not contribute to the marginal bone resorption in either group.* Int J Oral Maxillofac Implants 2008;23:335–342

Key words: *animal study, histomorphometry, machined neck, marginal bone level, microbial leakage, rough neck*

The replacement of missing teeth by means of endosseous titanium implants has become an evidence-based treatment modality for both completely and partially edentulous patients.[1–4] This concept is mainly based on the biologic phenomenon of osseointegration, defined as direct structural and functional connection between ordered, living bone and the surface of a load-bearing implant.[5] Predictable treatment outcomes have been reported for both submerged[6] and nonsubmerged healing procedures.[7–11] The formation of peri-implant tissues is not dependent on the surgical approach.[12–14] Indeed, the transmucosal attachment at submerged and nonsubmerged implants reveals a junctional epithelium and connective tissue resulting in a 3- to 4-mm-wide zone of soft tissue coverage of the implant-supporting bone.[15,16] However, distinct crestal bone changes of about 2 mm have been reported in the first year of loading, particularly around 2-piece implants.[17,18] In recent years, several investigations have examined these initial crestal bone changes. In particular, some authors have examined the potential role of the microgap at the implant-abutment interface in bacterial colonization of the implant sulcus.[19–21] Biologic

[1]Assistant Professor, Department of Oral Surgery, Heinrich Heine University, Düsseldorf, Germany.
[2]Research Associate, Department of Oral Surgery, Heinrich Heine University, Düsseldorf, Germany.
[3]Professor and Chairman, Department of Oral Surgery, Heinrich Heine University, Düsseldorf, Germany.

Correspondence to: Dr Frank Schwarz, Department of Oral Surgery, Westdeutsche Kieferklinik, Heinrich Heine University, D-40225 Düsseldorf, Germany. Fax: +49 211 1713542. E-mail: info@frank-schwarz.de

aspects such as the formation of a proper biological width,[22] biomechanical aspects such as interfacial shear strength,[23] and the influence of the implant design itself (eg, macro- and microstructure) have also been discussed.[24,25] Due to the fact that rough surfaces accumulate and retain more plaque than smooth surfaces, nowadays, most implant systems use machined implant necks.[26–28] However, Zechner et al observed significantly more long-term periimplant bone loss with machined implants compared to rough-surfaced implants.[25] Moreover, Jung et al observed a correlation between the amount of bone resorption and the length of the machined neck (ie, the longer the machined neck, the greater the bone resorption).[29] The optimal ratio of machined surface to roughened surface at the implant neck is still unknown. Therefore, the aim of the present study was to histomorphometrically investigate crestal bone changes at nonsubmerged implants with different machined collar lengths in a dog model.

MATERIALS AND METHODS

Animals

Four beagle dogs (age, 20 to 24 months; mean weight, 16.4 ± 0.4 kg) were used in the study. All animals exhibited a fully erupted permanent dentition. During the experiment, the dogs were fed once per day with soft food and water. Animal selection, management, and surgery protocol were approved by the Animal Care and Use Committee of Heinrich Heine University and the Bezirksregierung Düsseldorf. The experimental segment of the study started after an adaption period of 4 weeks.

Study Design

The study was performed in 2 surgical phases. In the first phase, extraction of the mandibular and maxillary second, third, and fourth premolars and first molar (P2 to M1) was performed bilaterally. After 4 months of healing, surgical implantation of screw-type sandblasted and acid-etched (Promote; Camlog, Basel, Switzerland) implants (3.8 mm wide, 11 mm long, Camlog Screw Line) was performed in a nonsubmerged healing procedure (phase 2). Both test implants (machined neck size: 0.4 mm, commercial name Promote plus; CAM+) and control implants (machined neck size: 1.6 mm; CAM) implants were randomly assigned to the mandibles according to a split-mouth design; each animal received 2 implants per group. Standard abutments (width of 3.8 mm, height of 4 mm, Camlog) were connected with a torque of 15 Ncm immediately following implant placement in both groups.

There was no prosthesis load on the implants. Randomization was performed according to a computer-generated list (RandList, DatInf, Tübingen, Germany). Accordingly, each animal received 4 implants bilaterally in the mandible (2 CAM, 2 CAM+, respectively). Radiographs were obtained before and immediately after tooth extraction as well as immediately after implant insertion. The animals were sacrificed after healing periods of 2 and 12 weeks (2 animals per period).

Surgical Procedure

After sedation with acepromazine (0.17 mg/kg body weight), the dogs were anesthetized with 21.5 mg/kg thiopental sodium. For all surgical procedures, inhalation anesthesia was performed with oxygen, nitrous oxide, and isoflurane. To maintain hydration, all animals received a constant rate infusion of lactated Ringer solution while anesthetized. In the first surgery, P2 to M1 were carefully removed bilaterally in both jaws after reflection of mucoperiosteal flaps and tooth separation. After wound closure by means of mattress sutures, the sites were allowed to heal for 4 months. Prophylactic administration of clindamycin (11.0 mg/kg body weight, Cleorobe; Pharmacia Tiergesundheit, Erlangen, Germany) was performed intra- and postoperatively for 10 days. In the second surgery, bilateral buccal incisions were made, and mucoperiosteal flaps were reflected to expose the respective sites for implant insertion in the mandibles. Surgical implant sites were prepared bilaterally at a distance of 10 mm apart using a low-trauma surgical technique under copious irrigation with sterile 0.9% physiologic saline. Both CAM and CAM+ implants were inserted so that the implant shoulder was situated 0.4 mm above the alveolar crest, as suggested by the surgical protocol of the manufacturer. Accordingly, in the CAM group, the machined neck was located approximately 1.1 mm subcrestally, whereas at CAM+ implants the machined neck was located at the bone crest level (Fig 1). Following connection of the standard abutments, wound closure was achieved with consecutive resorbable 5.0 polyglycolic acid sutures (Resorba, Nürnberg, Germany), and implants were left to heal in a transgingival position.

Retrieval of Specimens

The animals were sacrificed (overdose of sodium pentobarbital 3%) after healing periods of 2 and 12 weeks, respectively, and the oral tissues were fixed by perfusion with 10% buffered formalin administered through the carotid arteries. The jaws were dissected, and blocks containing the experimental specimens were obtained. All specimens were fixed in 10% neutral buffered formalin solution for 4 to 7 days.

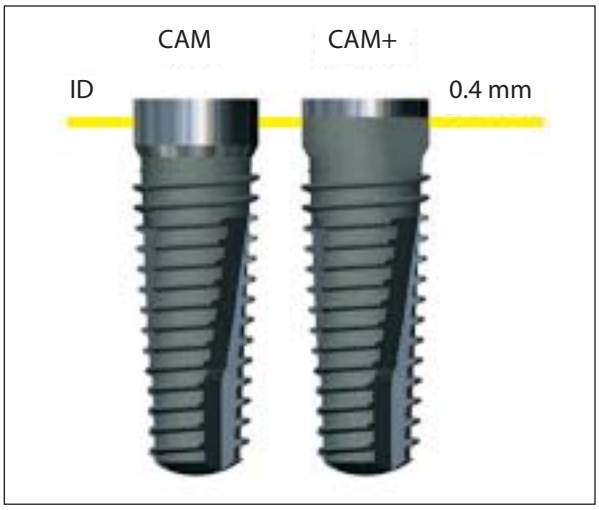

Fig 1 Both CAM and CAM+ implants were inserted so that the implant shoulder (IC) exceeded the alveolar crest for an insertion depth of 0.4 mm. Accordingly, in the CAM group, the machined neck was located approximately 1.1 mm subcrestally, whereas for CAM+ implants the machined neck was located at the bone crest level.

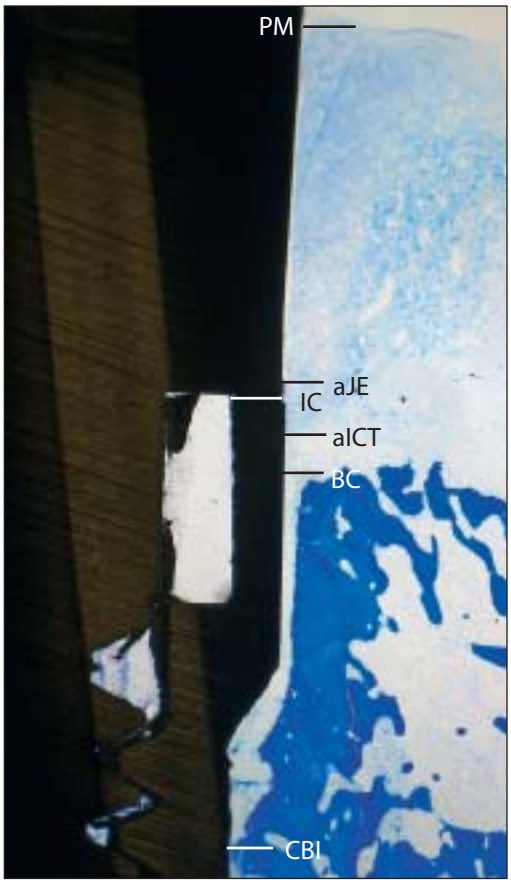

Fig 2 *(Right)* Landmarks for histomorphometric analysis. IC = the implant shoulder; PM = the marginal portion of the peri-implant mucosa; aJE = the apical extension of the long junctional epithelium; aICT = the apical extension of the inflammatory cell infiltrate; CBI = the most coronal level of bone in contact with the implant; BC = the level of the alveolar bone crest (CAM; toluidine blue, original magnification ×25).

Histologic Specimen Preparation

The specimens were dehydrated using ascending grades of alcohol and xylene, infiltrated, and embedded in methyl methacrylate (MMA, Technovit 7200; Heraeus Kulzer, Wehrheim, Germany) for nondecalcified sectioning. After 20 hours the specimens were completely polymerized. Each implant site was cut in the mesio-distal direction along with the long axis of the implant using a diamond wire saw (Exakt; Apparatebau, Norderstedt, Germany). Serial sections were prepared, resulting in 3 sections of approximately 500 µm in thickness.[30] Subsequently, all specimens were glued with acrylic resin cement (Technovit 7210 VLC; Heraeus Kulzer, Wehrheim, Germany) to opaque Plexiglas and ground to a final thickness of approximately 30 µm. All sections were stained with toluidine blue to evaluate marginal hard and soft tissue integration. With this technique, old bone stained light blue, whereas newly formed bone stained dark blue because of its higher protein content.[31]

Histologic Analysis

Histomorphometrical analyses as well as microscopic observations were performed by a single experienced investigator masked to the specific experimental conditions. For image acquisition a color CCD camera (Color View III; Olympus, Hamburg, Germany) was mounted on a binocular light microscope (Olympus BX50; Olympus, Hamburg, Germany). Digital images (original magnification ×200) were evaluated using a software program (analySIS FIVE docu, Soft Imaging System, Münster, Germany).

The following landmarks were identified in the stained sections at both mesial and distal aspects: the implant shoulder (IC), the marginal portion of the peri-implant mucosa (PM), the apical extension of the long junctional epithelium (aJE), the apical extension of the inflammatory cell infiltrate (aICT), the most coronal level of bone in contact with the implant (CBI), and the level of the alveolar bone crest (BC). The amount of new bone-to-implant contact (BIC) was measured as percentage of the distance ID-mesial to ID-distal (Fig 2).

Intraexaminer Reliability

Both microscopic observations and histomorphometric measurements were performed by a single experienced investigator masked to the specific experimental conditions. For histomorphometry, calibration was performed by means of 5 histologic sections. The

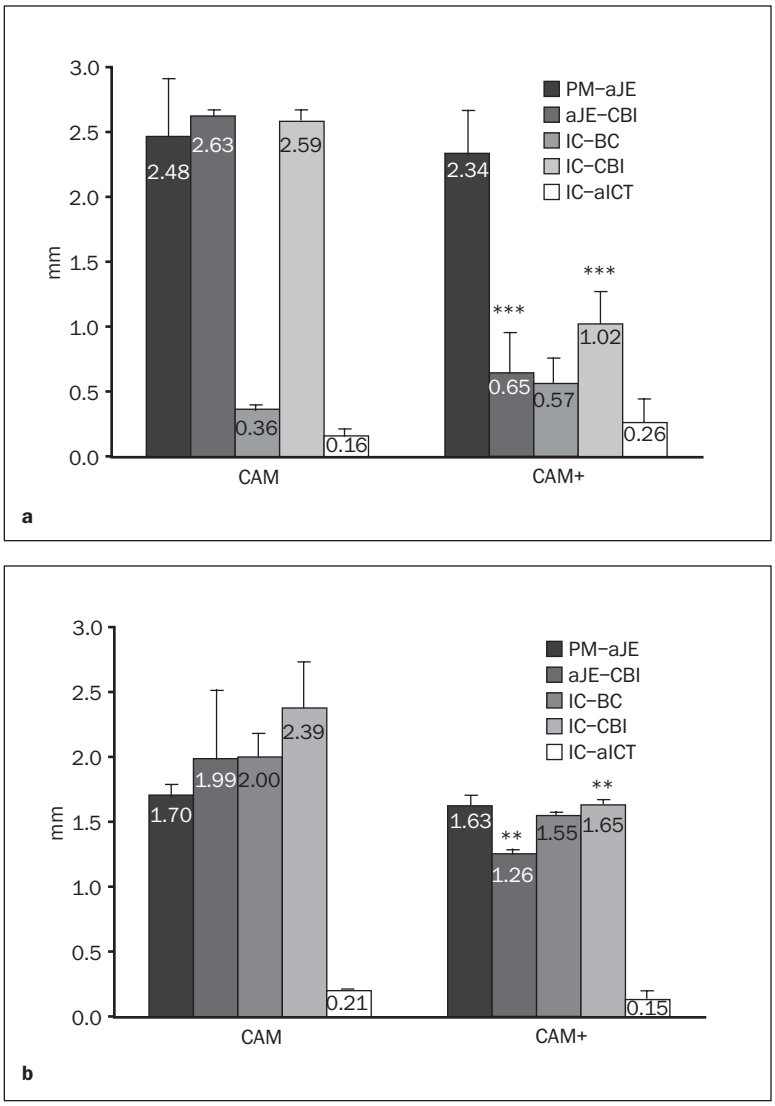

Fig 3 Histomorphometric parameters: Mean scores of PM-aJE, aJE-CBI, IC-BC, IC-CBI, and IC-aICT (in mm ± SD; n = 16 implants) in both groups after *(a)* 2 and *(b)* 12 weeks of healing. Comparisons between groups were made using the unpaired *t* test. ** $P < .01$; *** $P < .001$.

examiner evaluated the specimens on 2 separate occasions 48 hours apart. Calibration was accepted if measurements at baseline and at 48 hours were similar beyond an agreement level of 90%.

Statistical Analysis

The statistical analysis was performed using a commercially available software program (SPSS 14.0; SPSS, Chicago, IL). Mean values and standard deviations for peri-mucosa, the most coronal level of bone-implant contact, inflammatory cell infiltrate, and bone-implant contact were calculated for each group in each dog. The data rows were examined with the Kolmogorov-Smirnov test for normal distribution. For the statistical evaluation of the changes within groups over time, the paired *t* test was used. For comparisons between groups, the unpaired *t* test was used. The alpha error was set at .05.

RESULTS

Postoperative healing was generally uneventful in all dogs. No complications, such as allergic reactions, abscesses, or infections, were observed throughout the study period.

Histologic Observations/Histomorphometric Analysis

The mean values and percentages of PM-aJE, aJE-CBI, IC-BC, IC-CBI, IC-aICT, and BIC for each group at 2 and 12 weeks are presented in Figs 3 and 4.

In general, at 2 weeks following implant insertion, both CAM and CAM+ implants revealed comparable mean values of PM-aJE and IC-BC ($P > .05$, unpaired *t* test). Moreover, in both groups, mean IC-BC values appeared to be within the range of ID. However, histologic observation revealed obvious differences with respect to initial marginal bone adaptation in

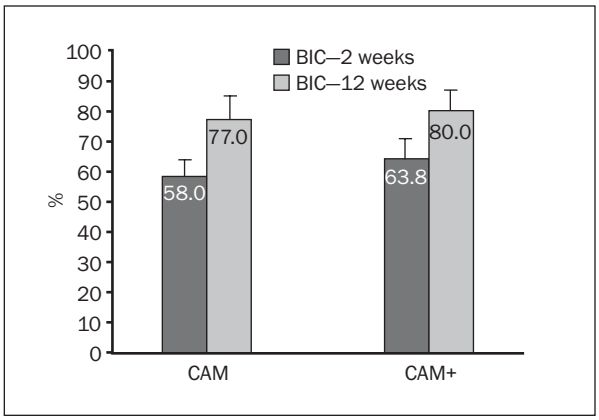

Fig 4 Histomorphometric parameters: Mean ± SD percentages of BIC (n = 16 implants) in both groups after 2 and 12 weeks of healing.

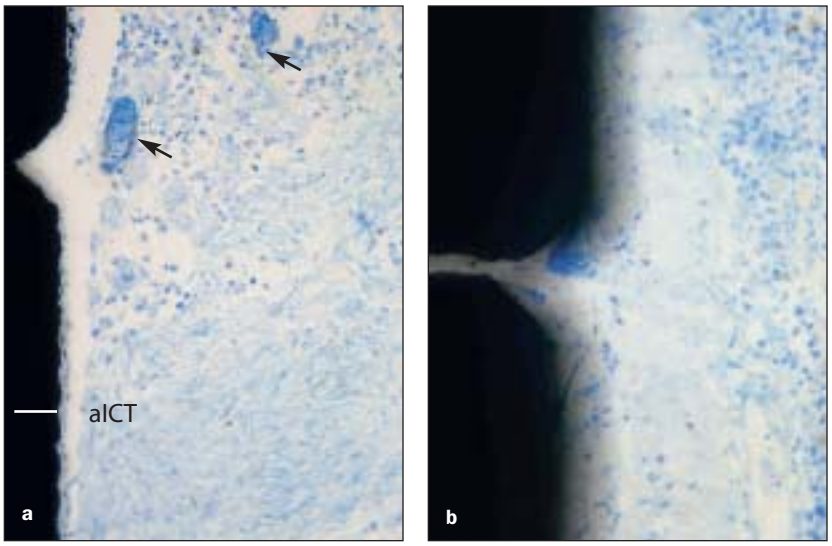

Fig 5 After 2 weeks of healing, inflammatory cell infiltrates were localized adjacent to the joint between the endosteal and transmucosal portion of both *(a)* CAM implants (toluidine blue; original magnification ×400) and *(b)* CAM+ implants (toluidine blue; original magnification ×500). Arrows indicate multinucleated giant cells. Extended gap formation is an artifact of histologic processing.

both groups. The marginal portion of CAM implants was separated from the parietal bone by a dense connective tissue zone (Fig 2). In contrast, CAM+ implants revealed CBI slightly apical to the level of ID, consisting of newly formed trabeculae of woven bone originating from the parietal alveolar bone. Accordingly, histomorphometric analysis revealed significantly higher mean values of both aJE-CBI and IC-CBI in the CAM group ($P < .001$, respectively, unpaired *t* test). In particular, while CBI was located at a mean distance of 2.6 ± 0.1 mm apical to IC in the CAM group, CAM+ implants revealed CBI at a mean distance of 1.0 ± 0.25 mm apical to IC ($P < .001$, unpaired *t* test). Similarly, aJE was generally located apical to IC in the CAM group, while aJE tended to be on a level with IC at CAM+ implants ($P < .001$, unpaired *t* test). Mean BIC values were comparable for the 2 groups ($P > .05$, unpaired *t* test; Fig 4). Histomorphometric analysis revealed a localized inflammatory cell infiltrate adjacent to the joint between the endosteal and transmucosal portion of both CAM and CAM+ implants, as indicated by low mean IC-aICT values ($P > .05$, unpaired *t* test). In both groups, aICT and BC were clearly separated by a subepithelial connective tissue zone with parallel running collagen fibers and rare blood vessel formation (Figs 5a and 5b). After 12 weeks, histologic analysis revealed ongoing bone formation within the endosteal area of both groups, as indicated by increased mean BIC values ($P < .001$, respectively, paired *t* test). In particular, both CAM and CAM+ implants seemed to be surrounded by firmly attached mature parallel-fibered woven bone (Figs 6a and 6b). However, histomorphometric analysis also revealed increased mean IC-BC values in both groups ($P < .001$, respectively, paired *t* test). While CAM implants exhibited significant decreased mean aJE-CBI and IC-CBI values, CAM+ implants revealed

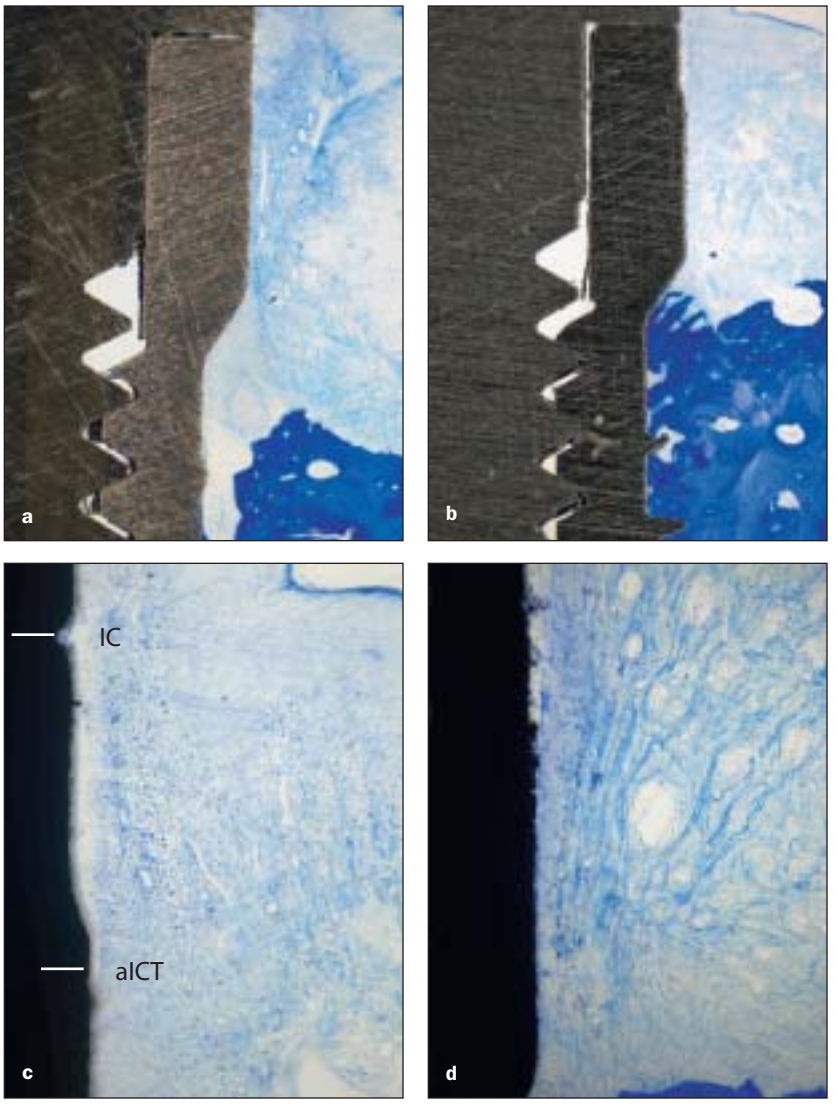

Fig 6 Histologic views of ongoing bone formation in the endosteal area of both groups. After 12 weeks of healing, *(a)* CAM and *(b)* CAM+ implants had undergone significant crestal bone loss. However, the rough-surfaced implant necks of CAM+ implants significantly reduced crestal bone level changes (toluidine blue; original magnification ×25). In both groups, the inflammatory cell infiltrate was clearly separated from the bone crest by a subepithelial connective tissue zone with parallel running collagen fibers and rare blood vessel formation. *(c)* CAM (toluidine blue; original magnification ×200). *(d)* CAM+ (toluidine blue stain, original magnification ×200).

significant increases of respective mean aJE-CBI and IC-CBI values ($P < .01$, respectively, paired *t* test; Figs 3a and 3b). Mean aJE-CBI and IC-CBI values were significantly lower at CAM+ implants ($P < .01$, respectively, paired *t* test). In both groups, histomorphometric analysis failed to reveal any increases of mean IC-aICT values after 12 weeks of healing ($P > .05$, respectively, paired *t* test; Figs 6c and 6d).

DISCUSSION

The present study was designed to histomorphometrically investigate crestal bone changes at nonsubmerged implants with different machined collar lengths in a dog model. Within the limits of the present study, it was observed that at 2 weeks, the machined neck of CAM implants interfered with the process of osseointegration. In contrast, CAM+ implants revealed newly formed trabeculae of woven bone in close contact with the implant neck. After 12 weeks of healing, however, both CAM and CAM+ implants exhibited a significant loss of the crestal bone, although statistical analysis revealed significantly higher values in the CAM group. When interpreting the present results, it was also observed that both CAM and CAM+ implants exhibited an ongoing bone formation in the endosteal area, as indicated by increased mean BIC values over time. Even though these are the first data investigating crestal bone changes at both types of implants after 2 and 12 weeks, mean BIC values noted for CAM implants

seemed to be within the range reported in a recent pilot study in dogs after 4 weeks of submerged healing.[32] There might be several possible reasons for the crestal bone changes in both groups. First of all, it must be emphasized that the mobilization of mucoperiosteal flaps might have caused an insult upon the periosteum and bone.[33] Secondly, several studies have reported microbial leakage resulting in a mucosal inflammatory reaction that might have influenced marginal bone resorption.[19–21] Indeed, the results of a previous in vitro study showed that CAM implants exhibited bacterial leakage along the implant-abutment interface. In this test model, *Escherichia coli* contamination was assessed under functional loading in an artificial chewing simulator.[34] This observation might also be supported by the results of the present study, since histomorphometric analysis revealed a slight inflammatory cell infiltrate in the connective tissue adjacent to the implant-abutment interface of both the CAM and CAM+ groups. However, after 2 and 12 weeks of healing, the inflammatory cell infiltrate was clearly separated from the implant supporting alveolar bone by a sound subepithelial connective tissue zone. Accordingly, it might be hypothesized that microbial leakage apparently did not contribute to the marginal bone resorption in either group. As described, Jung et al observed a correlation for the amount of marginal bone resorption and the length of the machined neck (ie, the longer the machined neck, the higher the bone resorption).[29] Shin et al also observed significantly greater marginal bone level changes at machined necks in comparison to rough-surfaced necks after 3, 6, and 12 months of healing.[24] Moreover, Hermann et al reported that implants with machined surfaces located below the bone crest level revealed significantly higher crestal bone changes.[35] All these data taken together with the results from the present study seem to indicate that the first bone-implant contact is dependent on the border between a rough and smooth implant surface. Indeed, many studies have clearly demonstrated that bone tissue favors rough implant surfaces compared to relatively smooth titanium surfaces.[36–40] When interpreting the present results, however, it must be realized that CAM+ implants also revealed significant crestal bone changes at 12 weeks. This might be explained by the concept of crestal bone loss due to the formation of a biological width.[22] In particular, the zone of connective tissue at CAM+ implants increased from 0.6 ± 0.3 mm at 2 weeks to 1.3 ± 0.1 mm at 12 weeks. This observation is in agreement with the results from a previous experimental study in dogs, which indicated that the peri-implant mucosa contained a zone of connective tissue that was about 1.3 to 1.8 mm high.[22]

CONCLUSIONS

Within the limits of the present study, it was concluded that *(1)* rough-surfaced implant necks reduced crestal bone level changes after 12 weeks of healing and *(2)* microbial leakage apparently did not contribute to the marginal bone resorption in either group.

ACKNOWLEDGMENTS

The authors appreciate the skills and commitment of Ms Brigitte Hartig and Mr Daniel Ferrari in the preparation of the histologic specimens. The study materials were kindly provided by Camlog, Basel, Switzerland.

REFERENCES

1. Buser D, Mericske-Stern R, Bernard JP, et al. Long-term evaluation of non-submerged ITI implants. Part 1: 8-year life table analysis of a prospective multi-center study with 2359 implants. Clin Oral Implants Res 1997;8:161–172.
2. Jemt T, Chai J, Harnett J, et al. A 5-year prospective multicenter follow-up report on overdentures supported by osseointegrated implants. Int J Oral Maxillofac Implants 1996;11:291–298.
3. Lambrecht JT, Filippi A, Kunzel AR, Schiel HJ. Long-term evaluation of submerged and nonsubmerged ITI solid-screw titanium implants: A 10-year life table analysis of 468 implants. Int J Oral Maxillofac Implants 2003;18:826–834.
4. Lindquist LW, Carlsson GE, Jemt T. A prospective 15-year follow-up study of mandibular fixed prostheses supported by osseointegrated implants. Clinical results and marginal bone loss. Clin Oral Implants Res 1996;7:329–336.
5. Brånemark PI. Introduction to osseointegration. In: Brånemark P-I, Zarb G, Albrektsson T (eds). Tissue-Integrated Prostheses: Osseointegration in Clinical Dentistry. Chicago: Quintessence, 1985:11–76.
6. Brånemark PI, Adell R, Breine U, Hansson BO, Lindstrom J, Ohlsson A. Intra-osseous anchorage of dental prostheses. I. Experimental studies. Scand J Plast Reconstr Surg 1969;3:81–100.
7. Becker W, Becker BE, Israelson H, et al. One-step surgical placement of Brånemark implants: A prospective multicenter clinical study. Int J Oral Maxillofac Implants 1997;12:454–462.
8. Bernard JP, Belser UC, Martinet JP, Borgis SA. Osseointegration of Brånemark fixtures using a single-step operating technique. A preliminary prospective one-year study in the edentulous mandible. Clin Oral Implants Res 1995;6:122–129.
9. Collaert B, De Bruyn H. Comparison of Brånemark fixture integration and short-term survival using one-stage or two-stage surgery in completely and partially edentulous mandibles. Clin Oral Implants Res 1998;9:131–135.
10. Ericsson I, Randow K, Glantz PO, Lindhe J, Nilner K. Clinical and radiographical features of submerged and nonsubmerged titanium implants. Clin Oral Implants Res 1994;5:185–189.
11. Henry P, Rosenberg I. Single-stage surgery for rehabilitation of the edentulous mandible: Preliminary results. Pract Periodontics Aesthet Dent 1994;6:15–22.
12. Abrahamsson I, Berglundh T, Wennstrom J, Lindhe J. The peri-implant hard and soft tissues at different implant systems. A comparative study in the dog. Clin Oral Implants Res 1996;7:212–219.

13. Ericsson I, Nilner K, Klinge B, Glantz PO. Radiographical and histological characteristics of submerged and nonsubmerged titanium implants. An experimental study in the Labrador dog. Clin Oral Implants Res 1996;7:20–26.
14. Weber HP, Buser D, Donath K, et al. Comparison of healed tissues adjacent to submerged and non-submerged unloaded titanium dental implants. A histometric study in beagle dogs. Clin Oral Implants Res 1996;7:11–19.
15. Berglundh T, Lindhe J, Ericsson I, Marinello CP, Liljenberg B, Thomsen P. The soft tissue barrier at implants and teeth. Clin Oral Implants Res 1991;2:81–90.
16. Fartash B, Arvidson K, Ericsson I. Histology of tissues surrounding single crystal sapphire endosseous dental implants: An experimental study in the beagle dog. Clin Oral Implants Res 1990;1:13–21.
17. Albrektsson T, Zarb G, Worthington P, Eriksson AR. The long-term efficacy of currently used dental implants: A review and proposed criteria of success. Int J Oral Maxillofac Implants 1986;1:11–25.
18. Smith DE, Zarb GA. Criteria for success of osseointegrated endosseous implants. J Prosthet Dent 1989;62:567–572.
19. Hermann JS, Schoolfield JD, Schenk RK, Buser D, Cochran DL. Influence of the size of the microgap on crestal bone changes around titanium implants. A histometric evaluation of unloaded non-submerged implants in the canine mandible. J Periodontol 2001;72:1372–1383.
20. Mombelli A, van Oosten MA, Schurch E Jr, Land NP. The microbiota associated with successful or failing osseointegrated titanium implants. Oral Microbiol Immunol 1987;2:145–151.
21. King GN, Hermann JS, Schoolfield JD, Buser D, Cochran DL. Influence of the size of the microgap on crestal bone levels in non-submerged dental implants: A radiographic study in the canine mandible. J Periodontol 2002;73:1111–1117.
22. Berglundh T, Lindhe J. Dimension of the peri-implant mucosa. Biological width revisited. J Clin Periodontol 1996;23:971–973.
23. Rangert B, Jemt T, Jorneus L. Forces and moments on Brånemark implants. Int J Oral Maxillofac Implants 1989;4:241–247.
24. Shin YK, Han CH, Heo SJ, Kim S, Chun HJ. Radiographic evaluation of marginal bone level around implants with different neck designs after 1 year. Int J Oral Maxillofac Implants 2006;21:789–794.
25. Zechner W, Trinkl N, Watzak G, et al. Radiologic follow-up of peri-implant bone loss around machine-surfaced and rough-surfaced interforaminal implants in the mandible functionally loaded for 3 to 7 years. Int J Oral Maxillofac Implants 2004;19:216–221.
26. Rimondini L, Fare S, Brambilla E, et al. The effect of surface roughness on early in vivo plaque colonization on titanium. J Periodontol 1997;68:556–562.
27. Bollen CM, Lambrechts P, Quirynen M. Comparison of surface roughness of oral hard materials to the threshold surface roughness for bacterial plaque retention: A review of the literature. Dent Mater 1997;13:258–269.
28. Siegrist BE, Brecx MC, Gusberti FA, Joss A, Lang NP. In vivo early human dental plaque formation on different supporting substances. A scanning electron microscopic and bacteriological study. Clin Oral Implants Res 1991;2:38–46.
29. Jung YC, Han CH, Lee KW. A 1-year radiographic evaluation of marginal bone around dental implants. Int J Oral Maxillofac Implants 1996;11:811–818.
30. Donath K. The diagnostic value of the new method for the study of undecalcified bones and teeth with attached soft tissue (Sage-Schliff [sawing and grinding] technique). Pathol Res Pract 1985;179:631–633.
31. Schenk RK, Olah AJ, Herrmann W. Preparation of calcified tissues for light microscopy. In: Dickson GR (ed). Methods of Calcified Tissue Preparation. Amsterdam: Elsevier, 1984:1–56.
32. Becker J, Kirsch A, Schwarz F, et al. Bone apposition to titanium implants biocoated with recombinant human bone morphogenetic protein-2 (rhBMP-2). A pilot study in dogs. Clin Oral Investig 2006;10:217–224.
33. Pihlström BL, McHugh RB, Oliphant TH, Ortiz-Campos C. Comparison of surgical and nonsurgical treatment of periodontal disease. A review of current studies and additional results after 6 1/2 years. J Clin Periodontol 1983;10:524–541.
34. Steinebrunner L, Wolfart S, Bossmann K, Kern M. In vitro evaluation of bacterial leakage along the implant-abutment interface of different implant systems. Int J Oral Maxillofac Implants 2005;20:875–881.
35. Hermann JS, Buser D, Schenk RK, Cochran DL. Crestal bone changes around titanium implants. A histometric evaluation of unloaded non-submerged and submerged implants in the canine mandible. J Periodontol 2000;71:1412–1424.
36. Larsson C, Thomsen P, Aronsson BO, et al. Bone response to surface-modified titanium implants: Studies on the early tissue response to machined and electropolished implants with different oxide thicknesses. Biomaterials 1996;17:605–616.
37. Wong M, Eulenberger J, Schenk R, Hunziker E. Effect of surface topology on the osseointegration of implant materials in trabecular bone. J Biomed Mater Res 1995;29:1567–1575.
38. Buser D, Schenk RK, Steinemann S, Fiorellini JP, Fox CH, Stich H. Influence of surface characteristics on bone integration of titanium implants. A histomorphometric study in miniature pigs. J Biomed Mater Res 1991;25:889–902.
39. Larsson C, Thomsen P, Lausmaa J, Rodahl M, Kasemo B, Ericson LE. Bone response to surface modified titanium implants: Studies on electropolished implants with different oxide thicknesses and morphology. Biomaterials 1994;15:1062–1074.
40. Piattelli A, Scarano A, Piattelli M, Calabrese L. Direct bone formation on sand-blasted titanium implants: An experimental study. Biomaterials 1996;17:1015–1018.